Black hole shadow in a general rotating spacetime obtained through Newman-Janis algorithm

Rajibul Shaikh[*]
Department of Physics, Indian Institute of Technology, Kanpur 208016, India

(Received 22 April 2019; published 15 July 2019)

The Newman-Janis (NJ) algorithm has been extensively used in the literature to generate rotating black hole solutions from nonrotating seed spacetimes. In this work, we show, using various constants of motion, that the null geodesic equations in an arbitrary stationary and axially symmetric rotating spacetime obtained through the NJ algorithm can be separated completely, provided that the algorithm is applied successfully without any inconsistency. Using the separated null geodesic equations, we then obtain an analytic general formula for obtaining the contour of a shadow cast by a compact object whose gravitational field is given by the arbitrary rotating spacetime under consideration. As special cases, we apply our general analytic formula to some known black holes and reproduce the corresponding results for black hole shadow. Finally, we consider a new example and study shadow using our analytic general formula.

DOI: 10.1103/PhysRevD.100.024028

I. INTRODUCTION

It is generally believed that the central supermassive compact region of our Galaxy and those of many other galaxies contain supermassive black holes. Images and shadows formed due to gravitational lensing of light provide an observational tool in probing the gravitational fields around such compact objects and in detecting their nature. The gravitational field near a black hole event horizon becomes so strong that its exterior geometry can possesses unstable circular photon orbits or unstable light rings (or a photon sphere in the case of a spherically symmetric, static black hole) which causes photons to undergo unboundedly large amount of bending (strong gravitational lensing) [1–5]. A slight perturbation on photons on such unstable orbits can cause them to be either absorbed by the black hole or sent off to a faraway observer. Therefore, the event horizon of a black hole, together with the unstable light rings, is expected to create a characteristic shadowlike image (a darker region over a brighter background) of the photons emitted from nearby light sources or of the radiation emitted from an accretion flow around it. Very recently, the event horizon telescope (EHT) [6–8] has observed this shadow in the image of M87*. However, the observational outcome of the image of the supermassive compact object Sagittarius A* (Sgr A*) present at our Galactic center is yet to come.

While the intensity map of an image depends on the details of the emission mechanisms of photons, the contour (silhouette) of the shadow is determined only by the spacetime metric itself, since it corresponds to the apparent shape of the photon capture orbits (or the unstable light rings) as seen by a distant observer. Therefore, strong lensing images and shadows offer us an exciting opportunity not only to detect the nature of a compact object but also to test whether or not the gravitational field around a compact object is described by the Schwarzschild or Kerr geometry. In light of this, there have been both analytic and numerical efforts to investigate shadows cast by different black holes in the last few decades. The shadow of a Schwarzschild black hole was studied by Synge [9] and Luminet [10]. Bardeen studied the shadow cast by a Kerr black hole [11] (see [12] also). Consequently, the Kerr black hole shadow and its different aspects such as the measurement of the mass and spin parameter have been investigated by several authors [13–25]. The shadows cast by various other black holes have also been studied [26–71]. See [72] for a recent brief review on shadows. Some recent studies, however, suggest that the presence of a shadow does not by itself prove that a compact object is necessarily a black hole. Other horizonless compact objects, which posses light rings around them, can also cast shadows [73–88].

Unlike the nonrotating ones, rotating black hole solutions are very hard to obtain as exact solutions of the field equations of various gravity theories. On the other hand, the Newman-Janis (NJ) algorithm provides an easier and more useful way to generate a stationary and axisymmetric rotating black hole spacetime from a static and spherically symmetric nonrotating seed metric [89,90] (see [91,92] also). This method has been extensively used in the literature in recent times. In fact, many of the rotating black hole solutions cited above have been obtained through this method. The NJ method, however, has some

[*]rshaikh@iitk.ac.in

shortcomings and may not be useful in some cases to generate the rotating black hole metric. Another useful method to derive general parametrization of axisymmetric black holes can be found in [93,94]. In this work, we study shadow cast by a general rotating black hole generated from a nonrotating one through the NJ algorithm. A similar work has been considered in [95] in the case when the initial nonrotating seed black hole spacetime has a particular ansatz. However, our work here is not restricted to such an ansatz and deals with a most general rotating black hole generated through the NJ algorithm.

This paper is organized as follows. In the next section, we briefly summarize the NJ algorithm and apply it to obtain a most general rotating black hole spacetime from a nonrotating one. In Sec. III, we separate null geodesic equations in the general rotating black hole spacetime and obtain a general analytic formula for obtaining the contour of the shadow which the black hole cast. We apply our formula to verify some known results in Sec. IV. In Sec. V, we generate a new rotating black hole solution using the NJ algorithm and study its shadow. Finally, we conclude in Sec. VI.

II. ROTATING SPACETIME THROUGH NEWMAN-JANIS ALGORITHM

In this section, we briefly summarize the NJ algorithm described in [89,90] for the construction of a stationary and axisymmetric spacetime from a static and spherically symmetric one (see [91] also for more details). We start with the spherically symmetric, static spacetime given by

$$ds^2 = -f(r)dt^2 + \frac{dr^2}{g(r)} + h(r)(d\theta^2 + \sin^2\theta d\phi^2). \quad (1)$$

The first step of the algorithm is to write down the above metric in the advance null (Eddington-Finkelstein) coordinates (u, r, θ, φ) using the transformation,

$$du = dt - \frac{dr}{\sqrt{fg}}. \quad (2)$$

The metric in the advance null coordinates becomes

$$ds^2 = -f(r)du^2 - 2\sqrt{\frac{f}{g}}du dr + h(r)(d\theta^2 + \sin^2\theta d\phi^2). \quad (3)$$

The second step is to express the inverse metric $g^{\mu\nu}$ using a null tetrad $Z^\mu_\alpha = (l^\mu, n^\mu, m^\mu, \bar{m}^\mu)$ in the form

$$g^{\mu\nu} = -l^\mu n^\nu - l^\nu n^\mu + m^\mu \bar{m}^\nu + m^\nu \bar{m}^\mu, \quad (4)$$

where $\bar{m}^\mu$ is the complex conjugate of m^μ, and the tetrad vectors satisfy the relations,

$$l_\mu l^\mu = n_\mu n^\mu = m_\mu m^\mu = l_\mu m^\mu = n_\mu m^\mu = 0, \quad (5)$$

$$l_\mu n^\mu = -m_\mu \bar{m}^\mu = -1. \quad (6)$$

One finds that the tetrad vectors satisfying the above relations are given by

$$l^\mu = \delta^\mu_r, \qquad n^\mu = \sqrt{\frac{g}{f}}\delta^\mu_u - \frac{g}{2}\delta^\mu_r,$$
$$m^\mu = \frac{1}{\sqrt{2h}}\left(\delta^\mu_\theta + \frac{i}{\sin\theta}\delta^\mu_\phi\right). \quad (7)$$

The third step is a complex transformation in the $r - u$ plane given by

$$r \to r' = r + ia\cos\theta, \qquad u \to u' = u - ia\cos\theta, \quad (8)$$

together with the complexification of the metric functions $f(r)$, $g(r)$ and $h(r)$. After the complex transformation, the new tetrad vectors become

$$l'^\mu = \delta^\mu_r, \qquad n'^\mu = \sqrt{\frac{G(r,\theta)}{F(r,\theta)}}\delta^\mu_u - \frac{G(r,\theta)}{2}\delta^\mu_r, \quad (9)$$

$$m'^\mu = \frac{1}{\sqrt{2H(r,\theta)}}\left(ia\sin\theta(\delta^\mu_u - \delta^\mu_r) + \delta^\mu_\theta + \frac{i}{\sin\theta}\delta^\mu_\phi\right), \quad (10)$$

where $F(r,\theta)$, $G(r,\theta)$ and $H(r,\theta)$ are, respectively, the complexified form of $f(r)$, $g(r)$ and $h(r)$. Using the new tetrad, we find the new inverse metric using

$$g^{\mu\nu} = -l'^\mu n'^\nu - l'^\nu n'^\mu + m'^\mu \bar{m}'^\nu + m'^\nu \bar{m}'^\mu. \quad (11)$$

The new metric in the advance null coordinates becomes

$$ds^2 = -F du^2 - 2\sqrt{\frac{F}{G}}du dr + 2a\sin^2\theta\left(F - \sqrt{\frac{F}{G}}\right)du d\phi$$
$$+ 2a\sqrt{\frac{F}{G}}\sin^2\theta dr d\phi + H d\theta^2$$
$$+ \sin^2\theta\left[H + a^2\sin^2\theta\left(2\sqrt{\frac{F}{G}} - F\right)\right]d\phi^2. \quad (12)$$

The final step of the algorithm is to write down the metric in Boyer-Lindquist form (where the only nonzero off diagonal term is $g_{t\phi}$) using the coordinate transformations,

$$du = dt' + \chi_1(r)dr, \qquad d\phi = d\phi' + \chi_2(r)dr. \quad (13)$$

Inserting the above coordinate transformations in the metric (12) and setting $g_{t'r}$ and $g_{r\phi'}$ to zero, we obtain

$$\chi_1(r) = -\frac{\sqrt{\frac{G(r,\theta)}{F(r,\theta)}}H(r,\theta) + a^2\sin^2\theta}{G(r,\theta)H(r,\theta) + a^2\sin^2\theta}, \tag{14}$$

$$\chi_2(r) = -\frac{a}{G(r,\theta)H(r,\theta) + a^2\sin^2\theta}. \tag{15}$$

Note that the transformation in (13) is possible only when χ_1 and χ_2 depend only on r. If the right-hand sides of Eqs. (14) and (15) depend on θ also, then we cannot perform a global coordinate transformation of the form (13) [92]. Although it is not always possible to find a suitable complexification of the functions in such a way that χ_1 and χ_2 are independent of θ, in many cases, it is. However, this involves a certain arbitrariness and an element of guess. There are many ways to complexify. Some are

$$\frac{1}{r} \to \frac{1}{2}\left(\frac{1}{r'} + \frac{1}{\bar{r}'}\right) = \frac{r}{\rho^2}, \qquad r^2 \to r'\bar{r}' = \rho^2, \tag{16}$$

where $\rho^2 = r^2 + a^2\cos^2\theta$. Finally, once the global coordinate transformation (13) is allowed, the metric in the Boyer-Lindquist coordinate becomes

$$\begin{aligned} ds^2 &= -Fdt^2 - 2a\sin^2\theta\left(\sqrt{\frac{F}{G}} - F\right)dtd\phi \\ &\quad + \frac{H}{GH + a^2\sin^2\theta}dr^2 + Hd\theta^2 \\ &\quad + \sin^2\theta\left[H + a^2\sin^2\theta\left(2\sqrt{\frac{F}{G}} - F\right)\right]d\phi^2, \end{aligned} \tag{17}$$

where we have dropped the prime sign from t' and ϕ'. For later use, we define

$$\Delta(r) = G(r,\theta)H(r,\theta) + a^2\sin^2\theta, \tag{18}$$

$$X(r) = \sqrt{\frac{G(r,\theta)}{F(r,\theta)}}H(r,\theta) + a^2\sin^2\theta. \tag{19}$$

From Eqs. (14) and (15), note that Δ and X must be independent of θ so that the transformation (13) is allowed.

III. SEPARATION OF NULL GEODESIC EQUATIONS AND BLACK HOLE SHADOW

In this section, we separate the null geodesic equations in the general rotating spacetime (17) using the Hamilton-Jacobi method and obtain a general formula for finding the contour of a shadow. The Hamilton-Jacobi equation is given by

$$\frac{\partial S}{\partial \lambda} + H = 0, \qquad H = \frac{1}{2}g_{\mu\nu}p^\mu p^\nu, \tag{20}$$

where λ is the affine parameter, S is the Jacobi action, H is the Hamiltonian, and p^μ is the momentum defined by

$$p_\mu = \frac{\partial S}{\partial x^\mu} = g_{\mu\nu}\frac{dx^\nu}{d\lambda}. \tag{21}$$

Since the metric tensor $g_{\mu\nu}$ and hence the Hamiltonian H is independent of the coordinates t and ϕ, we have two constants of motion. These are the conserved energy $E = -p_t$ and the conserved angular momentum $L = p_\phi$ (about the axis of symmetry). If there is a separable solution of Eq. (20), then, in terms of the already known constants of the motion, it must take the form,

$$S = \frac{1}{2}\mu^2\lambda - Et + L\phi + S_r(r) + S_\theta(\theta), \tag{22}$$

where μ is the mass of the test particle. For a photon, we take $\mu = 0$. Putting Eq. (22) in the Hamilton-Jacobi equation, we obtain after some simplifications,

$$\begin{aligned} &-(GH + a^2\sin^2\theta)\left(\frac{dS_r}{dr}\right)^2 + \frac{\left[\left(\sqrt{\frac{G}{F}}H + a^2\sin^2\theta\right)E - aL\right]^2}{(GH + a^2\sin^2\theta)} \\ &\quad -(L - aE)^2 = \left(\frac{dS_\theta}{d\theta}\right)^2 + L^2\cot^2\theta - a^2E^2\cos^2\theta. \end{aligned} \tag{23}$$

Note that, since the quantities $(GH + a^2\sin^2\theta)[=\Delta(r)]$ and $(\sqrt{\frac{G}{F}}H + a^2\sin^2\theta)[= X(r)]$ are functions of r only [see Eqs. (18) and (19)], the left- and right-hand side of Eq. (23) are only functions of r and θ, respectively. Therefore, each side must be equal to a separation constant. After separation, we obtain

$$\begin{aligned} &-(GH + a^2\sin^2\theta)\left(\frac{dS_r}{dr}\right)^2 + \frac{\left[\left(\sqrt{\frac{G}{F}}H + a^2\sin^2\theta\right)E - aL\right]^2}{(GH + a^2\sin^2\theta)} \\ &\quad -(L - aE)^2 = \mathcal{K}, \end{aligned} \tag{24}$$

$$\left(\frac{dS_\theta}{d\theta}\right)^2 + L^2\cot^2\theta - a^2E^2\cos^2\theta = \mathcal{K}, \tag{25}$$

where the separation constant $\mathcal{K}$ is known as the Carter constant. Using Eq. (21), we obtain the following separated geodesic equations for the photon:

$$\frac{F}{G}\Delta(r)\frac{dt}{d\lambda} = \left[H + a^2\sin^2\theta\left(2\sqrt{\frac{F}{G}} - F\right)\right]E - a\left(\sqrt{\frac{F}{G}} - F\right)L, \tag{26}$$

$$\frac{F}{G}\Delta(r)\sin^2\theta\frac{d\phi}{d\lambda} = a\sin^2\theta\left(\sqrt{\frac{F}{G}} - F\right)E + FL, \tag{27}$$

$$H\frac{dr}{d\lambda} = \pm\sqrt{R(r)}, \tag{28}$$

$$H\frac{d\theta}{d\lambda} = \pm\sqrt{\Theta(\theta)}, \tag{29}$$

where

$$R(r) = [X(r)E - aL]^2 - \Delta(r)[\mathcal{K} + (L - aE)^2], \tag{30}$$

$$\Theta(\theta) = \mathcal{K} + a^2E^2\cos^2\theta - L^2\cot^2\theta, \tag{31}$$

and $\Delta(r)$ and $X(r)$ are defined, respectively, in Eqs. (18) and (19). Note that $R(r)$ and $\Theta(\theta)$ must be non-negative; i.e., we must have

$$\frac{R(r)}{E^2} = [X(r) - a\xi]^2 - \Delta(r)[\eta + (\xi - a)^2] \geq 0, \tag{32}$$

$$\frac{\Theta(\theta)}{E^2} = \eta + (\xi - a)^2 - \left(\frac{\xi}{\sin\theta} - a\sin\theta\right)^2 \geq 0 \tag{33}$$

for the photon motion, where $\xi = L/E$ and $\eta = \mathcal{K}/E^2$.

The unstable circular photon orbits in the general rotating spacetime must satisfy $R(r_{ph}) = 0$, $R'(r_{ph}) = 0$ and $R'' \geq 0$, where $r = r_{ph}$ is the radius of the unstable photon orbit. The first two conditions give

$$[X(r_{ph}) - a\xi]^2 - \Delta(r_{ph})[\eta + (\xi - a)^2] = 0, \tag{34}$$

$$2X'(r_{ph})[X(r_{ph}) - a\xi] - \Delta'(r_{ph})[\eta + (\xi - a)^2] = 0. \tag{35}$$

After eliminating η from the last two equations and solving for ξ, we obtain

$$\xi = \frac{X(r_{ph})}{a} \quad \text{or} \quad \xi = \frac{X(r_{ph})\Delta'(r_{ph}) - 2\Delta(r_{ph})X'(r_{ph})}{a\Delta'(r_{ph})}. \tag{36}$$

Out of these two solutions for ξ, only one is valid for the purpose of describing a black hole shadow. If we take the first solution $\xi = X/a$, then from Eq. (34), we find that the corresponding solution for η is given by

$$\eta + (\xi - a)^2 = 0, \tag{37}$$

which is compatible with the requirement $\Theta(\theta) \geq 0$ [see Eq. (33)] only for

$$\theta = \theta_{ph} = \text{a constant}, \quad \text{and} \quad \xi = a\sin^2\theta_{ph}, \tag{38}$$

when $\Theta(\theta) = 0$ for $\theta = \theta_{ph}$. This case is similar to the one of the cases of the Kerr black hole [12]. This set of solutions for ξ and η represents principal null-geodesics and can not describe a black hole shadow. Therefore, to describe a black hole shadow, we consider the second solution of ξ given in Eq. (36). Using this second solution, we solve for η from Eq. (35). We obtain

$$\xi = \frac{X_{ph}\Delta'_{ph} - 2\Delta_{ph}X'_{ph}}{a\Delta'_{ph}}, \tag{39}$$

$$\eta = \frac{4a^2X'^2_{ph}\Delta_{ph} - [(X_{ph} - a^2)\Delta'_{ph} - 2X'_{ph}\Delta_{ph}]^2}{a^2\Delta'^2_{ph}}, \tag{40}$$

where the subscript "ph" indicates that the quantities are evaluated at $r = r_{ph}$. Equations (39) and (40) give the general expressions for the critical impact parameters ξ and η of the unstable photon orbits which describe the contour of a shadow.

A particular case of the above study with

$$f(r) = g(r) = 1 - \frac{2m(r)}{r}, \qquad h(r) = r^2 \tag{41}$$

has been considered in [95]. In this case, using (16), the metric functions can be complexified to obtain [92]

$$F = G = 1 - \frac{2m(r)r}{\rho^2}, \qquad H = \rho^2, \qquad \rho^2 = r^2 + a^2\cos\theta^2. \tag{42}$$

Therefore, $\Delta(r)$ and $X(r)$ become

$$\Delta(r) = r^2 - 2m(r)r + a^2, \qquad X(r) = r^2 + a^2, \tag{43}$$

which are functions of r only. Using Eqs. (42) and (43), it is straightforward to show that the geodesic equations (26)–(29) as well as the expressions for ξ and η given in Eqs. (39) and (40) exactly match with those obtained in [95]. However, in our most general case here, we do not restrict the metric functions to be of the form given in Eq. (41).

The unstable photon orbits form the boundary of a shadow. The apparent shape of a shadow are obtained by using the celestial coordinates α and β which lie in the celestial plane perpendicular to the line joining the observer and the center of the spacetime geometry. The coordinates α and β are defined by [96]

$$\alpha = \lim_{r_0\to\infty}\left(-r_0^2\sin\theta_0\frac{d\phi}{dr}\bigg|_{(r_0,\theta_0)}\right), \tag{44}$$

$$\beta = \lim_{r_0\to\infty}\left(r_0^2\frac{d\theta}{dr}\bigg|_{(r_0,\theta_0)}\right), \tag{45}$$

where (r_0, θ_0) are the position coordinates of the observer. We consider that the general metric is asymptotically flat.

Therefore, $F \sim 1$, $G \sim 1$, $H \sim r^2$, $\Delta \sim r^2$ and $X \sim r^2$ in the limit $r \to \infty$. After taking the limit, we obtain

$$\alpha = -\frac{\xi}{\sin\theta_0}, \tag{46}$$

$$\beta = \pm\sqrt{\eta + a^2\cos^2\theta_0 - \xi^2\cot^2\theta_0}. \tag{47}$$

The shadows are constructed by using the unstable photon orbit radius r_{ph} as a parameter and then plotting parametric plots of α and β using Eqs. (39), (40), (46) and (47).

IV. SOME KNOWN EXAMPLES

A. Kerr, Kerr-Newman, and tidally charged rotating braneworld black hole

The Kerr [89,97], the Kerr-Newman [90] and the tidally charged rotating braneworld black hole [98] are, respectively, rotating solutions of Einstein-vacuum equations, Einstein-Maxwell equations and the effective field equations of the Randall-Sundrum braneworld in vacuum. Through the NJ algorithm, these black hole solutions can be obtained from the nonrotating metric given by

$$f(r) = g(r) = 1 - \frac{2M}{r} + \frac{q}{r^2}, \qquad h(r) = r^2, \tag{48}$$

where $q = 0$ represents Schwarzschild black hole, $q = Q^2$ represents electrically charged Reissner-Nordstrom black hole with Q being the electric charge, and $q = -Q_*^2$ represents tidally charged braneworld black hole with Q_* being the tidal charge. Using (16), the metric functions in this case can be complexified as [89,90]

$$F = G = 1 - \frac{2Mr}{\rho^2} + \frac{q}{\rho^2}, \qquad H = \rho^2, \qquad \rho^2 = r^2 + a^2\cos^2\theta. \tag{49}$$

Using these complexified functions in Eqs. (18) and (19), we obtain

$$\Delta(r) = r^2 - 2Mr + a^2 + q, \qquad X(r) = r^2 + a^2. \tag{50}$$

The black hole horizons are given by $\Delta = 0$. When $(M^2 - a^2 - q) \geq 0$, we have Kerr black hole for $q = 0$, Kerr-Newman black hole for $q = Q^2$ and tidally charged braneworld black hole for $q = -Q_*^2$. The shadows cast by these black holes have already been studied [11,32–34,50]. Using the above expression for $\Delta(r)$ and $X(r)$ in Eqs. (39) and (40), we obtain

$$\xi = \frac{2r_{ph}(2Mr_{ph} - q) - (r_{ph} + M)(r_{ph}^2 + a^2)}{a(r_{ph} - M)}, \tag{51}$$

$$\eta = \frac{4a^2 r_{ph}^2(Mr_{ph} - q) - r_{ph}^2[r_{ph}(r_{ph} - 3M) + 2q]^2}{a^2(r_{ph} - M)^2}, \tag{52}$$

which are the same as those of the Kerr ($q = 0$), Kerr-Newman ($q = Q^2$) and tidally charged braneworld black hole ($q = -Q_*^2$) obtained, respectively, in [11,33,50]. Note that the authors in [50] have taken $q = Q$ with $Q < 0$ for the tidally charged braneworld black hole.

B. Kerr-Sen black hole

The Kerr-Sen black hole is a rotating charged black hole solution obtained in heterotic string theory [99]. In [100], the author has shown that, using the NJ algorithm, the Kerr-Sen black hole solution can be obtained from the spherically symmetric, static metric given by

$$f(r) = g(r) = \frac{1 - \frac{r_1}{r}}{1 + \frac{r_2}{r}}, \qquad h(r) = r^2\left(1 + \frac{r_2}{r}\right), \tag{53}$$

where r_1 and r_2 are related to the mass M and the electric charge Q by $r_1 + r_2 = 2M$ and $r_2 = Q^2/M$. Note however that M and Q in [99] are related to the two parameters m and α by $M = (m/2)(1 + \cosh\alpha)$ and $Q = (m/\sqrt{2})\sinh\alpha$. In this case, using (16), the metric functions can be complexified as [100]

$$F = G = \frac{1 - \frac{r_1 r}{\rho^2}}{1 + \frac{r_2 r}{\rho^2}}, \quad H = \rho^2\left(1 + \frac{r_2 r}{\rho^2}\right), \quad \rho^2 = r^2 + a^2\cos^2\theta. \tag{54}$$

Therefore, $\Delta(r)$ and $X(r)$ in this case become

$$\Delta(r) = r^2 - r_1 r + a^2, \qquad X(r) = r^2 + r_2 r + a^2. \tag{55}$$

The shadows for this black hole have been studied in [39]. Using the last equation in Eqs. (39) and (40), we obtain

$$\xi = \frac{(r_1 + r_2)(r_{ph}^2 - a^2) - (2r_{ph} + r_2)(r_{ph}^2 - r_1 r_{ph} + a^2)}{a(2r_{ph} - r_1)}, \tag{56}$$

$$\eta = \frac{r_{ph}^2}{a^2(2r_{ph} - r_1)^2}\{4a^2(r_1 + r_2)(2r_{ph} + r_2) - [(2r_{ph} + r_2)(r_{ph} - r_1) - (r_1 + r_2)r_{ph}]^2\}. \tag{57}$$

We find that the above expressions for the critical impact parameters ξ and η are the same as those obtained in Eq. (27) of [39], after we replace $r_2 = r_0$ and $r_1 = 2M - r_0$ in the above expressions for ξ and η.

V. A NEW EXAMPLE: ROTATING DILATON BLACK HOLE AND ITS SHADOW

We now consider a new example to bring out the usefulness of our general analytic formula for obtaining a shadow. We consider the nonrotating charged dilaton black hole given by [101,102]

$$f(r) = g(r) = \frac{(1-\frac{r_-}{r})(1-\frac{r_+}{r})}{1-\frac{r_0^2}{r^2}}, \qquad h(r) = r^2\left(1-\frac{r_0^2}{r^2}\right), \tag{58}$$

$$r_\pm = M \pm \sqrt{M + r_0^2 - Q_E^2 - Q_M^2}, \qquad r_0 = \frac{Q_M^2 - Q_E^2}{2M}, \tag{59}$$

and apply the NJ algorithm to obtain the corresponding rotating charged dilaton black hole. Here, M is the mass, and Q_E, Q_M and r_0 are, respectively, related to the electric, the magnetic and the dilaton charge. To complexify the function, we first write $f(r)$ and $g(r)$ as

$$f(r) = g(r) = \frac{(1-\frac{2M}{r}+\frac{q}{r^2})}{1-\frac{r_0^2}{r^2}}, \tag{60}$$

where we have replaced $(r_- + r_+) = 2M$ and have defined $q = r_- r_+ = (Q_E^2 + Q_M^2 - r_0^2)$. Using (16), we now complexify the functions in the following way:

$$F = G = \frac{(1-\frac{2Mr}{\rho^2}+\frac{q}{\rho^2})}{1-\frac{r_0^2}{\rho^2}}, \qquad H = \rho^2\left(1-\frac{r_0^2}{\rho^2}\right),$$

$$\rho^2 = r^2 + a^2\cos^2\theta. \tag{61}$$

Using above equations, we find that the expressions for $\Delta(r)$ and $X(r)$ become

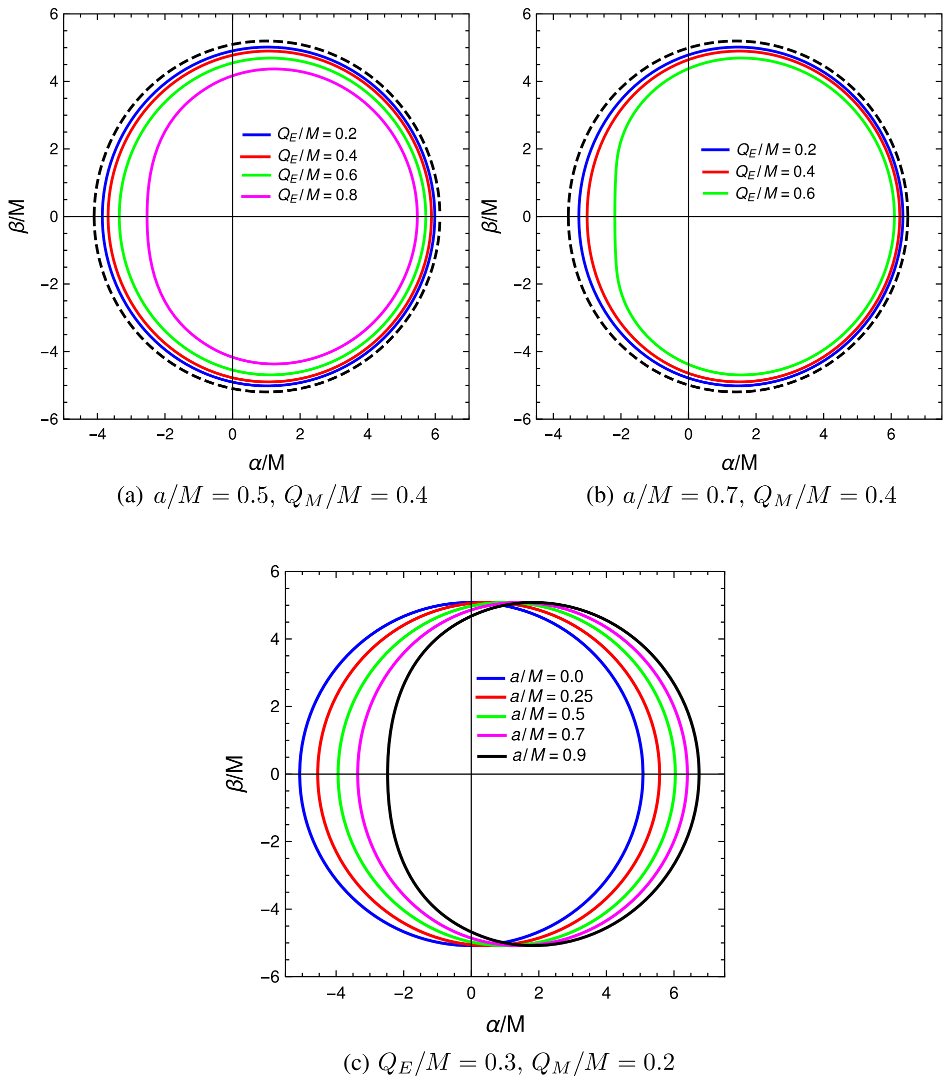

FIG. 1. Shadows cast by a rotating charged dilaton black hole for different parameter values [(a)–(c)]. The dashed contours are for a Kerr black hole with the spin values shown in the corresponding plot. The inclination angle of the observer is $\theta_0 = \pi/2$.

$$\Delta(r) = r^2 - 2Mr + a^2 + q, \qquad X(r) = r^2 - r_0^2 + a^2. \qquad (62)$$

Therefore, the critical impact parameters of the null geodesics in this case become

$$\xi = \frac{2r_{ph}(2Mr_{ph} - q) - r_0^2(r_{ph} - M) - (r_{ph} + M)(r_{ph}^2 + a^2)}{a(r_{ph} - M)}, \qquad (63)$$

$$\eta = \frac{1}{a^2(r_{ph} - M)^2}\{4a^2 r_{ph}^2(Mr_{ph} - q) - 4a^2 r_0^2 r_{ph}(r_{ph} - M) - [r_{ph}^2(r_{ph} - 3M) + 2qr_{ph} + r_0^2(r_{ph} - M)]^2\}. \qquad (64)$$

Note that when $Q_E = Q_M$, i.e., $r_0 = 0$, the dilaton charge vanishes, and the above results match with those of the Kerr-Newman black hole obtained in the previous section. To the best of our knowledge, construction of the above rotating metric using the NJ algorithm and its shadows have not been considered before. Figure 1 shows the shadows cast by the above rotating dilaton black hole for different values of the parameters.

VI. CONCLUSIONS

After the very recent observation of the very first image of the black hole M87* [6–8], a black hole shadow will continue to be an important probe of spacetime structure and gravity in the strong curvature regime. In this work, we have studied the shadow cast by an arbitrary stationary, axially symmetric and asymptotically flat rotating black hole spacetime generated through the NJ algorithm. To this end, we have completely separated the null geodesic equations using different constants of motion and obtained an analytic general formula which can be used to find the contour of the shadow cast by a rotating black hole. To demonstrate the usefulness of our general analytic formula, we have applied it to some known examples and reproduced the corresponding results. Finally, we have considered a new example and studied its shadows. Our analytic formula will be useful to obtain more new results for black hole shadows. Though we have applied our analytic formula to study shadows cast by rotating black holes, it can also be used to study shadows cast by other compact objects.

[1] K. S. Virbhadra and G. F. R. Ellis, Schwarzschild black hole lensing, Phys. Rev. D **62**, 084003 (2000).

[2] V. Bozza, S. Capozziello, G. Iovane, and G. Scarptta, Strong field limit of black hole gravitational lensing, Gen. Relativ. Gravit. **33**, 1535 (2001).

[3] V. Bozza, Gravitational lensing in the strong field limit, Phys. Rev. D **66**, 103001 (2002).

[4] V. Bozza, Gravitational lensing by black holes, Gen. Relativ. Gravit. **42**, 2269 (2010).

[5] R. Shaikh, P. Banerjee, S. Paul, and T. Sarkar, An analytical approach to strong gravitational lensing from ultra-compact objects, Phys. Rev. D **99**, 104040 (2019).

[6] The Event Horizon Telescope Collaboration, First M87 event horizon telescope results. I. The shadow of the supermassive black hole, Astrophys. J. Lett. **875**, L1 (2019).

[7] The Event Horizon Telescope Collaboration, First M87 event horizon telescope results. V. Physical origin of the asymmetric ring, Astrophys. J. Lett. **875**, L5 (2019).

[8] The Event Horizon Telescope Collaboration, First M87 event horizon telescope results. VI. The shadow and mass of the central black hole, Astrophys. J. Lett. **875**, L6 (2019).

[9] J. L. Synge, The escape of photons from gravitationally intense stars, Mon. Not. R. Astron. Soc. **131**, 463 (1966).

[10] J.-P. Luminet, Image of a spherical black hole with thin accretion disk, Astron. Astrophys. **75**, 228 (1979).

[11] J. M. Bardeen, in *Black Holes (Les Astres Occlus)*, edited by C. Dewitt and B. S. Dewitt (Gordon and Breach, New York, 1973), pp. 215–239.

[12] S. Chandrasekhar, *The Mathematical Theory of Black Holes* (Oxford University Press, New York, 1998).

[13] H. Falcke, F. Melia, and E. Agol, Viewing the shadow of the black hole at the galactic center, Astrophys. J. **528**, L13 (2000).

[14] R. Takahashi, Shapes and positions of black hole shadows in accretion disks and spin parameters of black holes, Astrophys. J. **611**, 996 (2004).

[15] A. F. Zakharov, A. A. Nucita, F. De Paolis, and G. Ingrosso, Measuring the black hole parameters in the galactic center with RADIOASTRON, New Astron. **10**, 479 (2005).

[16] K. Beckwith and C. Done, Extreme gravitational lensing near rotating black holes, Mon. Not. R. Astron. Soc. **359**, 1217 (2005).

[17] A. E. Broderick and A. Loeb, Frequency-dependent shift in the image centroid of the black hole at the galactic center as a test of general relativity, Astrophys. J. **636**, L109 (2006).

[18] R. Takahashi and K. Y. Watarai, Eclipsing light curves for accretion flows around a rotating black hole and atmospheric effects of the companion star, Mon. Not. R. Astron. Soc. **374**, 1515 (2007).

[19] K. Hioki and K.-I. Maeda, Measurement of the Kerr spin parameter by observation of a compact object's shadow, Phys. Rev. D **80**, 024042 (2009).

[20] T. Johannsen and D. Psaltis, Testing the no-hair theorem with observations in the electromagnetic spectrum. II. black hole images, Astrophys. J. **718**, 446 (2010).

[21] F. De Paolis, G. Ingrosso, A. A. Nucita, A. Qadir, and A. F. Zakharov, Estimating the parameters of the Sgr A* black hole, Gen. Relativ. Gravit. **43**, 977 (2011).

[22] G. V. Kraniotis, Precise analytic treatment of Kerr and Kerr-(anti) de Sitter black holes as gravitational lenses, Classical Quantum Gravity **28**, 085021 (2011).
[23] Z. Stuchlik, D. Charbulak, and J. Schee, Light escape cones in local reference frames of Kerr-de Sitter black hole spacetimes and related black hole shadows, Eur. Phys. J. C **78**, 180 (2018).
[24] R. Kumar and S. G. Ghosh, Black hole parameters estimation from its shadow, arXiv:1811.01260.
[25] S. W. Wei, Y. C. Zou, Y. X. Liu, and R. B. Mann, Curvature radius and Kerr black hole shadow, arXiv:1904.07710.
[26] A. F. Zakharov, F. De Paolis, G. Ingrosso, and A. A. Nucita, Direct measurements of black hole charge with future astrometrical missions, Astron. Astrophys. **442**, 795 (2005).
[27] A. F. Zakharov, Constraints on a charge in the Reissner-Nordstrom metric for the black hole at the Galactic Center, Phys. Rev. D **90**, 062007 (2014).
[28] Z. Stuchlik and J. Schee, Shadow of the regular Bardeen black holes and comparison of the motion of photons and neutrinos, Eur. Phys. J. C **79**, 44 (2019).
[29] A. Yumoto, D. Nitta, T. Chiba, and N. Sugiyama, Shadows of multi-black holes: Analytic exploration, Phys. Rev. D **86**, 103001 (2012).
[30] J. O. Shipley and S. R. Dolan, Binary black hole shadows, chaotic scattering and the Cantor set, Classical Quantum Gravity **33**, 175001 (2016).
[31] H. Gott, D. Ayzenberg, N. Yunes, and A. Lohfink, Observing the shadows of stellar-mass black holes with binary companions, Classical Quantum Gravity **36**, 055007 (2019).
[32] P. J. Young, Capture of particles from plunge orbits by a black hole, Phys. Rev. D **14**, 3281 (1976).
[33] A. de Vries, The apparent shape of a rotating charged black hole, closed photon orbits and the bifurcation set A_4, Classical Quantum Gravity **17**, 123 (2000).
[34] R. Takahashi, Black hole shadows of charged spinning black holes, Publ. Astron. Soc. Jpn. **57**, 273 (2005).
[35] G. V. Kraniotis, Gravitational lensing and frame dragging of light in the Kerr-Newman and the Kerr-Newman-(anti) de Sitter black hole spacetimes, Gen. Relativ. Gravit. **46**, 1818 (2014).
[36] J. W. Moffat, Modified gravity black holes and their observable shadows, Eur. Phys. J. C **75**, 130 (2015).
[37] A. Held, R. Gold, and A. Eichhorn, Asymptotic safety casts its shadow, arXiv:1904.07133.
[38] P. V. P. Cunha, C. A. R. Herdeiro, E. Radu, and H. F. Runarsson, Shadows of Kerr Black Holes with Scalar Hair, Phys. Rev. Lett. **115**, 211102 (2015).
[39] K. Hioki and U. Miyamoto, Hidden symmetries, null geodesics, and photon capture in the Sen black hole, Phys. Rev. D **78**, 044007 (2008).
[40] S. Dastan, R. Saffari, and S. Soroushfar, Shadow of a Kerr-Sen dilaton-axion black hole, arXiv:1610.09477.
[41] S. Abdolrahimi, R. B. Mann, and C. Tzounis, Distorted local shadows, Phys. Rev. D **91**, 084052 (2015).
[42] Z. Li and C. Bambi, Measuring the Kerr spin parameter of regular black holes from their shadow, J. Cosmol. Astropart. Phys. 01 (2014) 041.
[43] A. Abdujabbarov, M. Amir, B. Ahmedov, and S. G. Ghosh, Shadow of rotating regular black holes, Phys. Rev. D **93**, 104004 (2016).
[44] M. Amir and S. G. Ghosh, Shapes of rotating nonsingular black hole shadows, Phys. Rev. D **94**, 024054 (2016).
[45] M. Sharif and S. Iftikhar, Shadow of a charged rotating non-commutative black hole, Eur. Phys. J. C **76**, 630 (2016).
[46] A. Saha, M. Modumudi, and S. Gangopadhyay, Shadow of a noncommutative geometry inspired Ayon Beato Garcia black hole, Gen. Relativ. Gravit. **50**, 103 (2018).
[47] S. W. Wei and Y. X. Liu, Observing the shadow of Einstein-Maxwell-Dilaton-Axion black hole, J. Cosmol. Astropart. Phys. 11 (2013) 063.
[48] A. Abdujabbarov, F. Atamurotov, Y. Kucukakca, B. Ahmedov, and U. Camci, Shadow of Kerr-Taub-NUT black hole, Astrophys. Space Sci. **344**, 429 (2013).
[49] A. Grenzebach, V. Perlick, and C. Lammerzahl, Photon regions and shadows of Kerr-Newman-NUT black holes with a cosmological constant, Phys. Rev. D **89**, 124004 (2014).
[50] L. Amarilla and E. F. Eiroa, Shadow of a rotating brane-world black hole, Phys. Rev. D **85**, 064019 (2012).
[51] E. F. Eiroa and C. M. Sendra, Shadow cast by rotating braneworld black holes with a cosmological constant, Eur. Phys. J. C **78**, 91 (2018).
[52] L. Amarilla and E. F. Eiroa, Shadow of a Kaluza-Klein rotating dilaton black hole, Phys. Rev. D **87**, 044057 (2013).
[53] P. V. P. Cunha, C. A. R. Herdeiro, B. Kleihaus, J. Kunz, and E. Radu, Shadows of Einstein-dilaton-Gauss-Bonnet black holes, Phys. Lett. B **768**, 373 (2017).
[54] F. Atamurotov, A. Abdujabbarov, and B. Ahmedov, Shadow of rotating Horava-Lifshitz black hole, Astrophys. Space Sci. **348**, 179 (2013).
[55] F. Atamurotov, A. Abdujabbarov, and B. Ahmedov, Shadow of rotating non-Kerr black hole, Phys. Rev. D **88**, 064004 (2013).
[56] M. Wang, S. Chen, and J. Jing, Shadow casted by a Konoplya-Zhidenko rotating non-Kerr black hole, J. Cosmol. Astropart. Phys. 10 (2017) 051.
[57] H. M. Wang, Y. M. Xu, and S. W. Wei, Shadows of Kerr-like black holes in a modified gravity theory, J. Cosmol. Astropart. Phys. 03 (2019) 046.
[58] A. Ovgun, I. Sakalli, and J. Saavedra, Shadow cast and deflection angle of Kerr-Newman-Kasuya spacetime, J. Cosmol. Astropart. Phys. 10 (2018) 041.
[59] X. Hou, Z. Xu, and J. Wang, Rotating black hole shadow in perfect fluid dark matter, J. Cosmol. Astropart. Phys. 12 (2018) 040.
[60] S. Haroon, M. Jamil, K. Jusufi, K. Lin, and R. B. Mann, Shadow and deflection angle of rotating black holes in perfect fluid dark matter with a cosmological constant, Phys. Rev. D **99**, 044015 (2019).
[61] S. Haroon, K. Jusufi, and M. Jamil, Shadow images of a rotating dyonic black hole with a global monopole surrounded by perfect fluid, arXiv:1904.00711.
[62] V. Perlick, O. Y. Tsupko, and G. S. Bisnovatyi-Kogan, Black hole shadow in an expanding universe with a cosmological constant, Phys. Rev. D **97**, 104062 (2018).

[63] A. K. Mishra, S. Chakraborty, and S. Sarkar, Understanding photon sphere and black hole shadow in dynamically evolving spacetimes, Phys. Rev. D **99**, 104080 (2019).
[64] U. Papnoi, F. Atamurotov, S. G. Ghosh, and B. Ahmedov, Shadow of five-dimensional rotating Myers-Perry black hole, Phys. Rev. D **90**, 024073 (2014).
[65] M. Amir, B. P. Singh, and S. G. Ghosh, Shadows of rotating five-dimensional charged EMCS black holes, Eur. Phys. J. C **78**, 399 (2018).
[66] A. A. Abdujabbarov, F. Atamurotov, N. Dadhich, B. J. Ahmedov, and Z. Stuchlik, Energetics and optical properties of 6-dimensional rotating black hole in pure Gauss-Bonnet gravity, Eur. Phys. J. C **75**, 399 (2015).
[67] F. Atamurotov, B. Ahmedov, and A. Abdujabbarov, Optical properties of black holes in the presence of a plasma: The shadow, Phys. Rev. D **92**, 084005 (2015).
[68] A. Abdujabbarov, B. Toshmatov, Z. Stuchlik, and B. Ahmedov, Shadow of the rotating black hole with quintessential energy in the presence of plasma, Int. J. Mod. Phys. D **26**, 1750051 (2017).
[69] A. A. Abdujabbarov, L. Rezzolla, and B. J. Ahmedov, A coordinate-independent characterization of a black hole shadow, Mon. Not. R. Astron. Soc. **454**, 2423 (2015).
[70] Z. Younsi, A. Zhidenko, L. Rezzolla, R. Konoplya, and Y. Mizuno, New method for shadow calculations: Application to parametrized axisymmetric black holes, Phys. Rev. D **94**, 084025 (2016).
[71] A. Held, R. Gold, and A. Eichhorn, Asymptotic safety casts its shadow, arXiv:1904.07133.
[72] P. V. P. Cunha and C. A. R. Herdeiro, Shadows and strong gravitational lensing: A brief review, Gen. Relativ. Gravit. **50**, 42 (2018).
[73] P. V. P. Cunha, C. A. R. Herdeiro, and M. J. Rodriguez, Does the black hole shadow probe the event horizon geometry?, Phys. Rev. D **97**, 084020 (2018).
[74] A. E. Broderick and R. Narayan, On the nature of the compact dark mass at the galactic center, Astrophys. J. **638**, L21 (2006).
[75] C. Bambi and K. Freese, Apparent shape of super-spinning black holes, Phys. Rev. D **79**, 043002 (2009).
[76] R. Shaikh, P. Kocherlakota, R. Narayan, and P. S. Joshi, Shadows of spherically symmetric black holes and naked singularities, Mon. Not. R. Astron. Soc. **482**, 52 (2019).
[77] C. Bambi, Can the supermassive objects at the centers of galaxies be traversable wormholes? The first test of strong gravity for mm/sub-mm very long baseline interferometry facilities, Phys. Rev. D **87**, 107501 (2013).
[78] T. Ohgami and N. Sakai, Wormhole shadows, Phys. Rev. D **91**, 124020 (2015).
[79] M. Azreg-Ainou, Confined-exotic-matter wormholes with no gluing effect–Imaging supermassive wormholes and black holes, J. Cosmol. Astropart. Phys. 07 (2015) 037.
[80] T. Ohgami and N. Sakai, Wormhole shadows in rotating dust, Phys. Rev. D **94**, 064071 (2016).
[81] R. Shaikh, P. Banerjee, S. Paul, and T. Sarkar, A novel gravitational lensing feature by wormholes, Phys. Lett. B **789**, 270 (2019).
[82] P. G. Nedkova, V. Tinchev, and S. S. Yazadjiev, Shadow of a rotating traversable wormhole, Phys. Rev. D **88**, 124019 (2013).
[83] A. Abdujabbarov, B. Juraev, B. Ahmedov, and Z. Stuchlik, Shadow of rotating wormhole in plasma environment, Astrophys. Space Sci. **361**, 226 (2016).
[84] R. Shaikh, Shadows of rotating wormholes, Phys. Rev. D **98**, 024044 (2018).
[85] G. Gyulchev, P. Nedkova, V. Tinchev, and S. Yazadjiev, On the shadow of rotating traversable wormholes, Eur. Phys. J. C **78**, 544 (2018).
[86] M. Amir, K. Jusufi, A. Banerjee, and S. Hansraj, Shadow images of Kerr-like wormholes, arXiv:1806.07782.
[87] F. H. Vincent, Z. Meliani, P. Grandclement, E. Gourgoulhon, and O. Straub, Imaging a boson star at the Galactic center, Classical Quantum Gravity **33**, 105015 (2016).
[88] A. B. Abdikamalov, A. A. Abdujabbarov, D. Malafarina, C. Bambi, and B. Ahmedov, A black hole mimicker hiding in the shadow: Optical properties of the γ metric, arXiv:1904.06207.
[89] E. T. Newman and A. I. Janis, Note on the Kerr spinning-particle metric, J. Math. Phys. (N.Y.) **6**, 915 (1965).
[90] E. T. Newman, R. Couch, K. Chinnapared, A. Exton, A. Prakash, and R. Torrence, Metric of a rotating, charged Mass, J. Math. Phys. (N.Y.) **6**, 918 (1965).
[91] S. P. Drake and P. Szekeres, Uniqueness of the Newman-Janis algorithm in generating the Kerr-Newman metric, Gen. Relativ. Gravit. **32**, 445 (2000).
[92] C. Bambi and L. Modesto, Rotating regular black holes, Phys. Lett. B **721**, 329 (2013).
[93] L. Rezzolla and A. Zhidenko, New parametrization for spherically symmetric black holes in metric theories of gravity, Phys. Rev. D **90**, 084009 (2014).
[94] R. Konoplya, L. Rezzolla, and A. Zhidenko, General parametrization of axisymmetric black holesin metric theories of gravity, Phys. Rev. D **93**, 064015 (2016).
[95] N. Tsukamoto, Black hole shadow in an asymptotically-flat, stationary, and axisymmetric spacetime: The Kerr-Newman and rotating regular black holes, Phys. Rev. D **97**, 064021 (2018).
[96] S. E. Vazquez and E. P. Esteban, Strong-field gravitational lensing by a Kerr black hole, Nuovo Cimento B **119**, 489 (2004).
[97] R. P. Kerr, Gravitational Field of a Spinning Mass as an Example of Algebraically Special Metrics, Phys. Rev. Lett. **11**, 237 (1963).
[98] A. N. Aliev and A. E. Gumrukcuoglu, Charged rotating black holes on a 3-brane, Phys. Rev. D **71**, 104027 (2005).
[99] A. Sen, Rotating Charged Black Hole Solution in Heterotic String Theory, Phys. Rev. Lett. **69**, 1006 (1992).
[100] S. Yazadjiev, Newman-Janis method and rotating dilaton axion black hole, Gen. Relativ. Gravit. **32**, 2345 (2000).
[101] G. Gibbons and K. Maeda, Black holes and membranes in higher-dimensional theories with dilaton fields, Nucl. Phys. **B298**, 741 (1988).
[102] R. Kallosh, A. Linde, T. Ortin, A. Peet, and A. Van Proeyen, Supersymmetry as a cosmic censor, Phys. Rev. D **46**, 5278 (1992).